

STARS

University of Central Florida
STARS

Faculty Bibliography 2010s

Faculty Bibliography

1-1-2010

Optical transmission properties of C-shaped subwavelength waveguides on silicon

O. Lopatiuk-Tirpak
University of Central Florida

J. Ma
University of Central Florida

S. Fathpour
University of Central Florida

Find similar works at: <https://stars.library.ucf.edu/facultybib2010>

University of Central Florida Libraries <http://library.ucf.edu>

This Article is brought to you for free and open access by the Faculty Bibliography at STARS. It has been accepted for inclusion in Faculty Bibliography 2010s by an authorized administrator of STARS. For more information, please contact STARS@ucf.edu.

Recommended Citation

Lopatiuk-Tirpak, O.; Ma, J.; and Fathpour, S., "Optical transmission properties of C-shaped subwavelength waveguides on silicon" (2010). *Faculty Bibliography 2010s*. 460.

<https://stars.library.ucf.edu/facultybib2010/460>



Optical transmission properties of C-shaped subwavelength waveguides on silicon

Cite as: Appl. Phys. Lett. **96**, 241109 (2010); <https://doi.org/10.1063/1.3455839>

Submitted: 02 March 2010 . Accepted: 27 May 2010 . Published Online: 16 June 2010

O. Lopatiuk-Tirpak, J. Ma, and S. Fathpour



View Online



Export Citation

ARTICLES YOU MAY BE INTERESTED IN

[Effects of hole depth on enhanced light transmission through subwavelength hole arrays](#)
Applied Physics Letters **81**, 4327 (2002); <https://doi.org/10.1063/1.1526162>

Applied Physics Reviews
Now accepting original research

2017 Journal
Impact Factor:
12.894

Optical transmission properties of C-shaped subwavelength waveguides on silicon

O. Lopatiuk-Tirpak,¹ J. Ma,¹ and S. Fathpour^{1,2,a)}

¹CREOL, The College of Optics and Photonics, University of Central Florida, Orlando, Florida 32816, USA

²School of Electrical Engineering and Computer Science, University of Central Florida, Orlando, Florida 32816, USA

(Received 2 March 2010; accepted 27 May 2010; published online 16 June 2010)

Optical properties of C-shaped subwavelength waveguides in metallic (silver) films on silicon substrates are studied in the range of 0.6–6 μm . Power throughput and resonant wavelengths of several transmission modes are studied by varying the waveguide length (or metal thickness). Among three types of transmission modes, the fundamental order of the Fabry–Perot-type mode was shown to attain remarkably high power throughputs (as high as 12). With optimized design of the aperture, the resonant wavelength of this mode occurs in the 1–2 μm wavelength range, suggesting that such apertures can be utilized to achieve plasmonic-enhanced silicon photonic devices at telecommunication wavelengths. © 2010 American Institute of Physics. [doi:10.1063/1.3455839]

Subwavelength apertures are promising candidates for many nanophotonics applications where a combination of high transmittance and subwavelength spot size is necessary.^{1,2} Among the possible configurations, C-shaped single apertures have certain advantages due to their compact structure, which does not require the presence of arrays^{1,3} or extensive corrugation.⁴ C-shaped apertures have been utilized in photodetectors,^{5,6} waveguides,^{7,8} and surface-emitting lasers.⁹ There have been a number of numerical studies addressing the transmission properties of C-shaped apertures.^{7,10} Most of them, however, studied free-standing apertures in metallic films. As we have shown in our earlier work,¹¹ the properties of the C-apertures are altered quite dramatically by the refractive index of its surrounding media. This means that while numerical simulations in vacuum suggest impressive intensity enhancements and extraordinary transmission, these findings cannot necessarily be expected to be realized experimentally when the aperture is fabricated on a substrate.

In this paper, we report the results of a numerical study of the transmission properties of a C-shaped aperture-waveguide in silver (Ag) metallic films on a silicon substrate. Particularly, it is intended to study the power throughput (PT) of various involved transmission modes in order to predict their impact on the performance of silicon nanophotonic devices (ultracompact photodetectors, nanoantennas, etc.) at telecommunication wavelengths.

The dimensions of the aperture used in this study are shown in the inset of Fig. 1. The choice of the lateral dimensions of the aperture was motivated by the ultimate goal of achieving highest possible PT at wavelengths relevant to telecommunication applications. The calculations were performed using the finite-integration method within the CST MICROWAVE SUITE. Optical properties of the Ag film were simulated by fitting the experimentally obtained dielectric constant values¹² to the Drude model.¹¹ The undoped silicon substrate is simply modeled as a dielectric with refractive index of 3.45 to facilitate interpreting the results. This as-

sumption is justified considering that silicon's optical loss and dispersion are small compared to that of silver in the wavelength range of interest. The remainder of the space, including the aperture cavity, is set to vacuum. The excitation source was a plane wave with the amplitude of 1 V/m, polarized along the y -axis in the inset of Fig. 1. It was assumed that the excitation impinges from vacuum onto the metallic aperture ($+z$ direction).

PT is defined as the ratio of total power at the exit surface to that impinging upon the physical area of the aperture.¹³ Total power at the exit was calculated by integrating half the real part of the normal component of the complex Poynting vector, S , over the entire x - y plane immediately adjacent to the metal-semiconductor interface (2 nm into silicon). This choice of the plane is only to facilitate the numerical calculation of PT, since only S_z is needed. In general, any arbitrary surface that encompasses the whole transmitting area in silicon gives the same result. It was indeed confirmed that the error due to neglecting the lateral energy

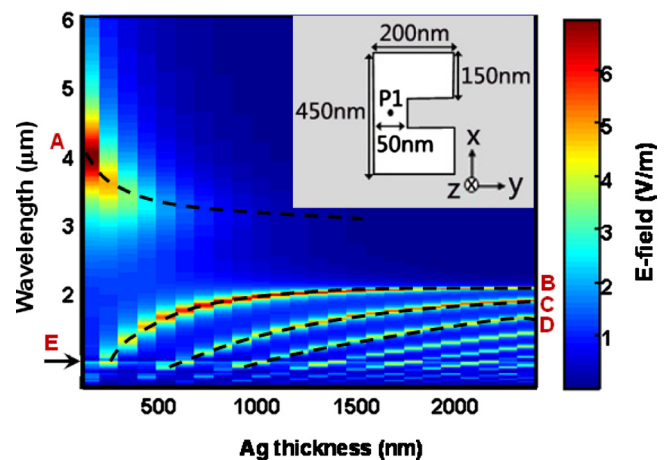


FIG. 1. (Color online) Spectral distribution of electric field magnitude as a function of the thickness of silver layer. The dashed lines indicate the evolution of the ESCP mode (A) and of the three orders of the FP mode (B, C, and D). The arrow indicates the spectral position of the SP mode (E). Inset: geometry and dimensions of the C-shaped aperture studied in this work.

^{a)}Electronic mail: fathpour@creol.ucf.edu.

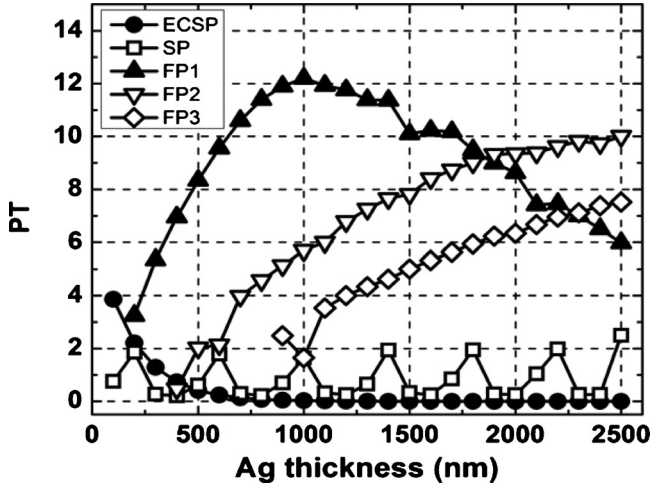


FIG. 2. PT vs metal layer thickness for the five transmission modes considered in this study.

flow—related to S_x and S_y in the very thin (2 nm) silicon layer adjacent to the metal—is negligible. This necessary clarification also applies to the same method of calculating PT in our earlier publication.¹¹

The evolution of spectral response with metal film thickness is shown in Fig. 1. The response is measured at point P1 in the inset of Fig. 1. The spectrum shows three different types of modes. They include: one evanescently coupled surface plasmon (ESCP) mode (denoted as A); one thickness-invariant surface plasmon (SP) mode associated with the substrate-metal interface at the wavelength of approximately 1 μm (denoted as E); and a Fabry–Perot (FP)-type cavity mode, showing an increasing number of orders with increased thickness (denoted as B, C, and D).¹¹

It is apparent from Fig. 1 that the change in the resonance wavelengths of the FP mode orders, λ_{FP} , is not linear with d (the FP cavity length), as might be expected for a true FP mode under ideal conditions. It must be pointed out that the wavelength of the FP resonances is determined not only by the thickness of the cavity but also by the phase change, ϕ , upon reflection from the front and back surfaces

$$\lambda_{\text{FP}} = 2d/(N - \phi/\pi), \quad (1)$$

where N is an integer.¹⁴ Therefore, the spectral position of the FP peaks can and does in this case differ considerably from $2d/N$.

The PT for each mode at its peak wavelength as a function of d was computed (Fig. 2). The ESCP mode is clearly evanescent in nature, since its PT decays exponentially with d . Although the transmittance via this mode may be somewhat high (and extraordinary, $\text{PT} \sim 4$) for small metal film thicknesses, it is not suitable for telecom applications, since the peak wavelength occurs in the 3.5–4 μm wavelength range (Fig. 1). The wavelength peak for this mode is indeed in the 1–2 μm range of interest and the PT can be even higher ($\text{PT} \sim 6$) if the substrate refractive index is close to 1, i.e., a free-standing apertures.¹¹ These observations on transmission properties of the ESCP mode in C-shaped apertures may explain the discrepancy between prediction of high PT in free-standing apertures¹⁰ and low performance of fabricated nanophotonic devices based on them (apertures on semiconductors).⁵

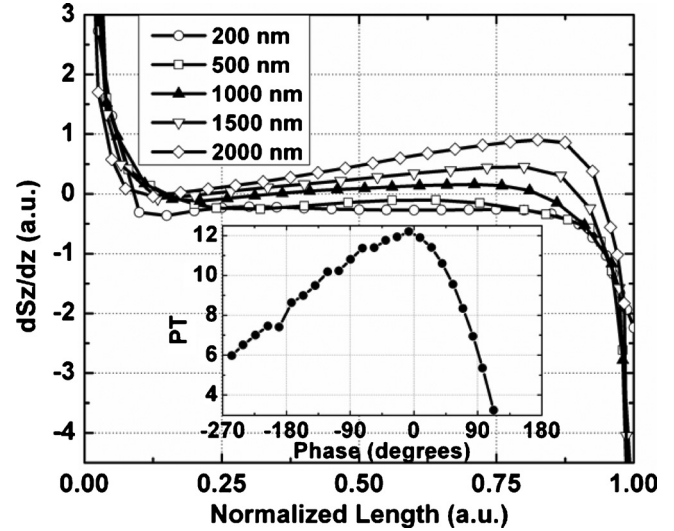


FIG. 3. Spatial distribution of the first derivative of the z -component of the Poynting vector along the direction of propagation, along the line containing point P1 in the inset of Fig. 1. Inset: PT as a function of phase [see Eq. (1)].

Another interesting finding of Fig. 2 is that the PT for the SP mode oscillates versus d with a nearly constant period (400 nm). Closer inspection and comparison of Figs. 1 and 2 reveals that the peaks in PT occur at the wavelengths of spectral overlap of SP and FP modes. As each successive order of the FP mode crosses the wavelength of the SP peak, both local intensity and PT of the SP mode increase sharply. Note that this same phenomenon has the opposite effect on the PT of the FP modes, i.e., it causes a sudden drop in the PT, particularly apparent at $d=600$ nm for FP2 (second order of the FP mode, open triangles in Fig. 2) and $d=1000$ nm for FP3 (open diamonds). The Poynting vector distribution at the wavelength of the FP mode acquires the symmetry characteristics of the SP, and a large fraction of power is scattered back toward the entrance surface.¹¹ The fact that PT of the SP mode peaks during such coupling indicates that the energy flow at these crossover wavelengths may have a hybrid character.

The most noteworthy result of this study is the behavior of the PT of the first order of the FP mode (FP1) of the aperture-waveguide. As shown in Fig. 2, by manipulating the thickness of the metal layer (i.e., waveguide length), PT values of nearly 12 can be achieved. Thus, it is important to focus on this fundamental FP mode for nanophotonic applications on real substrates rather than the tempting ESCP mode which appears to have modestly high PT but only in free-standing apertures. A high extraordinary PT of 12 for FP1 is due to the light-gathering ability of the subwavelength metal structure, where the energy incident onto the metal surface is captured in the form of surface plasmon waves and “funneled” via the waveguide FP-type mode.

The origin of the peak in the PT occurring at $d=1000$ nm in Fig. 2 may be related to the phase difference in Eq. (1). That is, the PT is maximal when the incident and reflected waves in the aperture cavity are in phase with each other. As mentioned before, varying the thickness of the metal layer affects both λ_{FP} and ϕ and therefore it is plausible that for a certain value of d this optimal condition can be achieved. Assuming $N=1$, for the fundamental FP mode, we calculated ϕ for every λ_{FP} (at each value of d) using Eq. (1) and found that PT indeed peaks when ϕ is close to zero

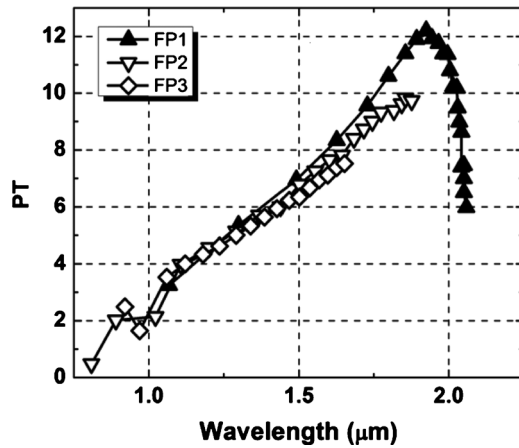


FIG. 4. Variation in PT with resonant wavelength for three orders of the FP mode.

(inset of Fig. 3). This finding is further supported by the spatial distribution of the PT for this mode. Figure 3 shows the normalized z -derivatives (through point P1) of the z -component of the Poynting vector, dS_z/dz , for five different values of d . This figure is intended to illustrate that for $d=1000$ nm (the thickness at which the peak in PT occurs), the spatial distribution is most uniform, i.e., $dS_z/dz \sim 0$. This is consistent with the minimal phase change upon reflection from the cavity surfaces. Furthermore, it is interesting to note that for all $d < 1000$ nm, the S_z slopes toward the entrance surface, while the opposite is true for $d > 1000$.

The two higher orders of the FP mode (FP2 and FP3) show similar tendencies and may peak as d is increased beyond 2500 nm. Figure 4 presents the PTs of the three FP modes as a function of peak wavelength, λ_{FP} . It is evident that although the PTs of different FP modes are different for the same waveguide lengths (see Fig. 2), the PTs show similar trends when plotted versus λ_{FP} . It is well-known that the reflectance of a FP cavity with fixed length is a periodic function of wavelength with the peaks corresponding to each successive order of the FP mode. In other words, the value of the reflectance at the peak wavelength of each FP order is the same. By increasing the cavity length (i.e., the metal film thickness) in the present case, higher FP orders can result in resonant wavelengths and hence reflectivities identical to those of the lower order(s) in thinner metal thicknesses (or shorter waveguides). Therefore, it is not surprising that

the variation in the reflectance (and hence the PT) is almost the same for all three FP orders when plotted versus λ_{FP} .

A PT of ~ 7 is predicted for FP1 at $\lambda_{FP}=1.55$ μm wavelength of telecommunication at $d=400$ nm. Similar PTs can be achieved at the higher FP2 and FP3 orders at the same wavelength, however at the expense of >1100 nm and >2000 nm metal thicknesses, respectively. Clearly, for this aperture geometry, only the FP1 mode renders itself to nanophotonic devices when practical thicknesses related to device fabrication issues are considered. Finally, it is noted that the highest PT of ~ 12 is predicted in Fig. 4 for the FP1 mode at the peak wavelength of $\lambda_{FP} \sim 1.92$ μm . Further optimization of the lateral geometry of the C-shaped nanoaperture can blueshift the PT in Fig. 4, in order to attain a maximal value in the telecommunication range of 1.3–1.55 μm .

In summary, this study shows that even under the conditions of refractive index mismatch between the aperture cavity and the substrate, high PT values can be achieved in C-shaped subwavelength aperture-waveguides in near-infrared wavelengths. For this purpose it is not only necessary to optimize the design of the aperture (both shape and thickness) but to also emphasize the FP-type modes.

This work was partially supported by the NASA Florida Space Grant Consortium under Award No. 16296041-Y5.

- ¹T. W. Ebbesen, H. J. Lezec, H. F. Ghaemi, T. Thio, and P. A. Wolff, *Nature (London)* **391**, 667 (1998).
- ²C. Genet and T. W. Ebbesen, *Nature (London)* **445**, 39 (2007).
- ³P. B. Catrysse and S. H. Fan, *J. Nanophotonics* **2**, 021790 (2008).
- ⁴F. J. García-Vidal, H. J. Lezec, T. W. Ebbesen, and L. Martin-Moreno, *Phys. Rev. Lett.* **90**, 213901 (2003); T. Thio, K. M. Pellerin, R. A. Linke, H. J. Lezec, and T. W. Ebbesen, *Opt. Lett.* **26**, 1972 (2001).
- ⁵L. Tang, D. A. B. Miller, A. K. Okyay, J. A. Matteo, Y. Yuen, K. C. Saraswat, and L. Hesselink, *Opt. Lett.* **31**, 1519 (2006).
- ⁶S.-X. Liu, P. An, Z.-Y. Zhang, Q. Zhang, L.-Q. Shen, and G.-Y. Jiang, *Electron. Lett.* **45**, 30 (2009).
- ⁷P. Hansen, L. Hesselink, and B. Leen, *Opt. Lett.* **32**, 1737 (2007).
- ⁸L. Y. Sun and L. Hesselink, *Opt. Lett.* **31**, 3606 (2006).
- ⁹Z. L. Rao, J. A. Matteo, L. Hesselink, and J. S. Harris, *Appl. Phys. Lett.* **90**, 191110 (2007).
- ¹⁰X. L. Shi and L. Hesselink, *J. Opt. Soc. Am. B* **21**, 1305 (2004); X. L. Shi, L. Hesselink, and R. L. Thornton, *Opt. Lett.* **28**, 1320 (2003).
- ¹¹O. Lopatiuk-Tirpak and S. Fathpour, *Opt. Express* **17**, 23861 (2009).
- ¹²M. A. Ordal, L. L. Long, R. J. Bell, S. E. Bell, R. R. Bell, R. W. Alexander, Jr., and C. A. Ward, *Appl. Opt.* **22**, 1099 (1983).
- ¹³J. Matteo and L. Hesselink, *Opt. Express* **13**, 636 (2005).
- ¹⁴Y. Pang, C. Genet, and T. W. Ebbesen, *Opt. Commun.* **280**, 10 (2007).